Earth and Planetary Science Letters 453 (2016) 67–77

Contents lists available at ScienceDirect

Earth and Planetary Science Letters

www.elsevier.com/locate/epsl

A silicon depleted North Atlantic since the Palaeogene: Evidence from sponge and radiolarian silicon isotopes

Guillaume Fontorbe [a,*], Patrick J. Frings [a], Christina L. De La Rocha [a], Katharine R. Hendry [b], Daniel J. Conley [a]

[a] Department of Geology, Lund University, Sölvegatan 12, SE-223 62, Lund, Sweden
[b] School of Earth Sciences, University of Bristol, Wills Memorial Building, Queen's Road, Bristol, BS8 1RJ, UK

ARTICLE INFO

Article history:
Received 23 November 2015
Received in revised form 1 August 2016
Accepted 4 August 2016
Available online xxxx
Editor: M. Frank

Keywords:
silicon isotopes
Palaeogene
radiolarians
sponges
ODP Leg 171B

ABSTRACT

Despite being one of Earth's major geochemical cycles, the evolution of the silicon cycle has received little attention and changes in oceanic dissolved silica (DSi) concentration through geologic time remain poorly constrained. Silicon isotope ratios (expressed as δ^{30}Si) in marine microfossils are becoming increasingly recognised for their ability to provide insight into silicon cycling. In particular, the δ^{30}Si of siliceous sponge spicules has been demonstrated to be a useful proxy for past DSi concentrations. We analysed δ^{30}Si in radiolarian tests and sponge spicules from the Blake Nose Palaeoceanographic Transect (ODP Leg 171B) spanning the Palaeocene–Eocene (ca. 60–30 Ma). Our δ^{30}Si results range from +0.32 to +1.67‰ and −0.48 to +0.63‰ for the radiolarian and sponge records, respectively. Using an established relationship between ambient dissolved Si (DSi) concentrations and the magnitude of silicon isotope fractionation in siliceous sponges, we demonstrate that the Western North Atlantic was DSi deplete during the Palaeocene–Eocene throughout the water column, a conclusion that is robust to a range of assumptions and uncertainties. These data can constitute constraints on reconstructions of past-ocean circulation. Previous work has suggested ocean DSi concentrations were higher than modern ocean concentrations prior to the Cenozoic and has posited a drawdown during the Early Palaeogene due to the evolutionary expansion of diatoms. Our results challenge such an interpretation. We suggest here that if such a global decrease in oceanic DSi concentrations occurred, it must predate 60 Ma.

1. Introduction

On geological time scales, the cycling of silicon (Si) is closely coupled to the climate system. Chemical weathering of silicate rocks converts atmospheric carbon dioxide (CO_2) to a fluvial alkalinity flux that is later precipitated as carbonate minerals in the ocean. This process counteracts a continuous CO_2 input from degassing of the solid Earth and so prevents excessive CO_2 accumulation in the atmosphere (Berner and Caldeira, 1997; Walker et al., 1981). The weathering of silicate rocks also releases solutes into continental ecosystems that will be ultimately transported to the ocean. Of these solutes, dissolved silica (DSi) is especially important for some marine organisms including diatoms, radiolarians and siliceous sponges that require silica to build their frustules, tests, or skeletons of biogenic silica (BSi). The biological uptake of dissolved silica and the subsequent precipitation as BSi imparts a fractionation to the silicon isotopes, with discrimination against the heavier Si isotopes, resulting in BSi with a lower proportion of the heavier isotopes than the DSi it originated from. Because burial of BSi is by far the main output of silica from the ocean (Tréguer and De La Rocha, 2013), the fractionation during biomineralisation of BSi has a significant influence over the distribution and cycling of silicon isotopes within the ocean.

Silicon isotope ratios (expressed as δ^{30}Si) in marine organisms have proven useful for reconstructions of different facets of the silica cycle, from nutrient use in surface waters (De La Rocha et al., 1998; Egan et al., 2012) to larger spatial and temporal scale changes in the marine silica cycle (De La Rocha, 2003). A recent development has been the use of δ^{30}Si of siliceous sponge spicules as a proxy for DSi concentrations in the ocean (Hendry and Robinson, 2012). Advantageously, the degree of Si isotope fractionation by siliceous sponges changes with ambient DSi concentration. This relationship has been used to reconstruct concentrations of DSi in past seawaters by making assumptions about the value of $\delta^{30}Si_{DSi}$, the isotopic composition of the ambient DSi (e.g. Griffiths et al., 2013). This is important, as DSi concentrations of bottom waters – where sponges grow – should be less sensitive to short term or

* Corresponding author.
E-mail address: guillaume.fontorbe@geol.lu.se (G. Fontorbe).

http://dx.doi.org/10.1016/j.epsl.2016.08.006

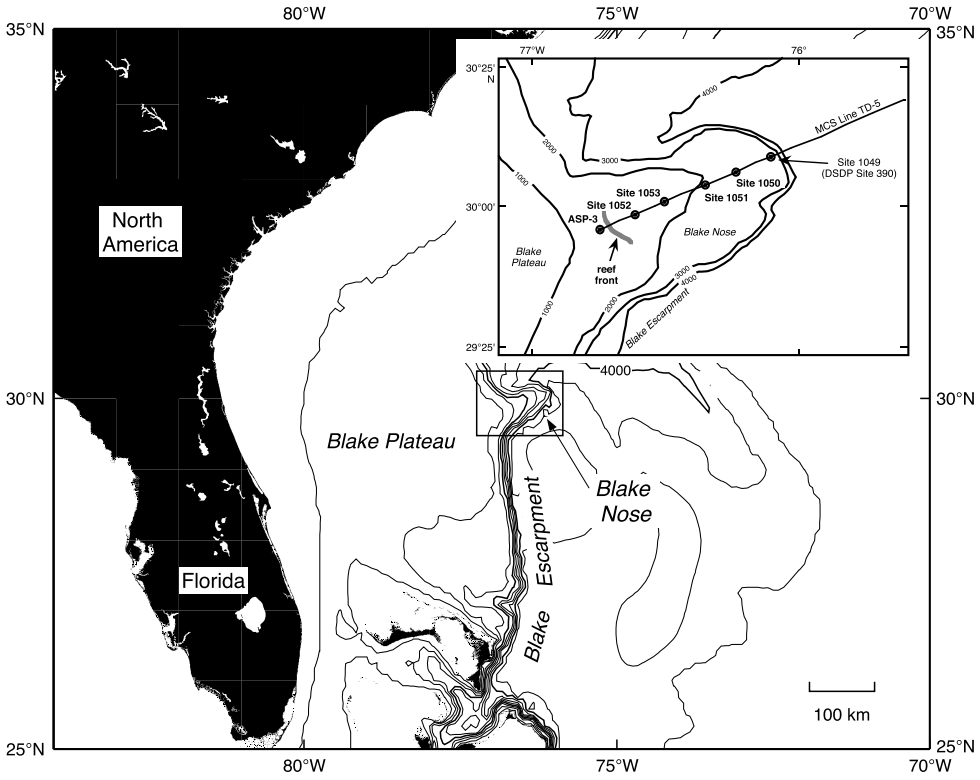

Fig. 1. Location of the drill sites in the Western North Atlantic. Modified from Norris et al. (1998).

local perturbations. Coupling the use of δ^{30}Si in sponge spicules to infer DSi concentrations with δ^{30}Si from other microfossils that instead reflect the δ^{30}Si of the waters they dwell in could be a profound but as yet relatively unexplored way to infer changes in the relationship between oceanic DSi concentrations, intensity of chemical weathering of silicate rocks and climate over geologic time.

Despite being one of the Earth's most fundamental geochemical cycles, the evolution of the oceanic Si cycle has received little attention. Ocean DSi concentrations over geological time have been estimated using the occurrences and facies distributions of cherts – microcrystalline quartz deposits – to define two end-member situations for the marine Si cycle: i. a Precambrian ocean characterised by saturation of DSi, and ii. the modern ocean characterised by DSi depletion at the surface (Maliva et al., 1989; Siever, 1992). In the absence of silica-secreting organisms, Precambrian DSi concentrations in the ocean must have reached saturation with respect to amorphous, hydrated silica, also known as opal (i.e. concentrations on the order of 1000–1800 µM). Ocean DSi was then brought below opal saturation following the evolution of the first silica-secreting organisms during the Neoproterozoic, with a final, more extreme drawdown towards modern conditions hypothesised in the late Cretaceous to early Cenozoic due to the rise of diatoms (Maliva et al., 1989).

This narrative raises questions about the timing and rate of the transition from a high DSi to a low DSi ocean, and whether it occurred as a single event or a series of stepwise changes. Also open to question is whether the net removal of silica from the ocean occurred because of an oceanwide increase in biologic silica production and export or if it was due to removal restricted to a small number of areas in the ocean. Developing the datasets necessary to answer these questions will further allow investigation into short and longer-term links between climate and the marine silica cycle.

One period to start tackling such questions is the Palaeogene (65.50–23.03 Ma). It encompasses the period of time when the diversification of diatoms is hypothesised to strengthen biological control over the ocean Si cycle (Maliva et al., 1989). Additionally, it allows us to study the behaviour of silicate weathering and the climate system under conditions 4 to 12 °C higher than modern temperatures (Zachos et al., 2001). Here, we investigate the evolution of the ocean Si cycle during the Palaeocene–Eocene as recorded in δ^{30}Si from siliceous sponge spicules and radiolarian tests in the Western North Atlantic Ocean (ODP Leg 171B). Using a published calibration to constrain ambient DSi concentrations in the deeper waters we show that DSi concentrations in the North Atlantic, which are remarkably low in the modern ocean, were already low during the Palaeocene–Eocene and probably had modern looking isotopic composition. This conclusion is robust to a range of reasonable δ^{30}Si values for the ambient DSi and adds substantial nuance to previous estimates of palaeo-DSi concentrations in the ocean.

2. Material and methods

2.1. Sample/site description

Samples from five cores (1049A, 1050A, 1051A, 1052A and 1053A) from the Blake Nose Palaeoceanographic Transect (ODP leg 171B; ca. 30°N, 76–77°W) were selected for analysis. Blake Nose is situated on the margin of the Blake Plateau (Fig. 1), where Palaeogene sediments are not extensively covered by more recent material and are topped by manganiferous sand and nodules that prevented post-depositional erosion (Norris et al., 2001). The cores have been drilled along a downslope transect spanning 1300–2700 mbsl.

Estimates of Paleocene–Eocene palaeodepths on Blake Nose vary between sources from water depths similar to present (Benson et al., 1978; Norris et al., 2001) to maximum estimations of water depths shallower by 1000 m compared to present based on foraminifera assemblages (Norris et al., 1998; Table 1). Even when taking into account the lowest possible palaeodepths (i.e. the shallowest estimates), the majority of the data presented in this study

Table 1
Hole locations, water depths, palaeodepths, sample intervals, approximate sampled age intervals, and number of analysed samples.

Hole	Location	Water depth (mbsl)	Palaeodepth (mbsl)	Sampled interval (mbsf)	Approx. age range (Ma)	Number of samples
1049 A	30°08.5436′N 76°06.7312′W	2667.3	1000–2000	33–70	39–50	8
1050 A	30°05.9977′N 76°14.1011′W	2299.8	1000–2000	36–294	41–60	28
1051 A	30°03.1740′N 76°21.4580′W	1982.7	1000–2000	15–610	34–59	27
1052 A	29°57.0906′N 76°37.5966′W	1344.5	600–1000	20–125	33–40	5
1053 A	29°59.5385′N 76°31.4135′W	1629.5	500–700	11–177	36–38	2

(90% of the total samples) comes from deposition depths below 1000 m. For clarity, in the rest of this study, we refer to this depth interval as "bottom waters" as opposed to "surface and intermediate waters" corresponding to the upper 1000 m characteristics of depths where radiolarians dwell.

The stratigraphic sequence in the cores is composed for the most part of Eocene carbonate ooze covering claystones from the Palaeocene and constitutes an almost complete sequence of Palaeocene–Eocene sediments. The age model we use derives from a mixture of foraminiferal and radiolarian biostratigraphy and magnetostratigraphy (Norris et al., 1998). Details of the cores and the sampled material can be found in Table 1. Modern day waters in this region are nearly entirely depleted in DSi at the surface, while DSi concentrations increase with depth up to about 30 µM at 3000 mbsl (Garcia et al., 2014). To our knowledge, no data exist for δ^{30}Si of DSi near Blake Nose. Reported values for δ^{30}Si of DSi offshore from Chesapeake Bay (ca. 37°N, 73°W) range from +1.5‰ near the surface to +0.9‰ at 3000 m depth, and between +1.2 and +1.5‰ between 1000 and 3000 m depth in the Sargasso Sea (31°N 58°W; De La Rocha et al., 2000).

2.2. Sample preparation

Biogenic silica was separated from other sediment fractions following the chemical and physical techniques detailed in Morley et al. (2004). Briefly, a few grams of bulk sediment were cleaned with hydrogen peroxide and hydrochloric acid to remove organic matter and carbonate material. BSi is separated from detrital material such as clays and other lithogenic silicates by repeated heavy liquid separation, using sodium polytungstate (SPT) at a density between 2.1 and 2.3 g/mL. The light fraction, containing the BSi, was then wet-sieved at 53 µm to isolate the larger fraction of BSi and remove the majority of fragmented material. From this, sponge spicules and radiolarian tests were handpicked under a light microscope to further minimise contamination. Only monoaxonic sponge spicules were collected to avoid the possible difference in silicon isotope fractionation between different types of sponge spicules (Hendry et al., 2015). It is important to note that given current poor understanding of radiolarian silicon isotope fractionation, we elected to pick the bulk radiolarian sample from the >53 µm fraction. Cleaned and separated BSi fractions were then dissolved in a large excess of HF. The resulting solution was diluted and purified via anion exchange chromatography following Engström et al. (2006) for isotopic analysis.

Silicon isotope ratios of the purified Si solutions were measured using a multi-collector inductively coupled plasma mass spectrometer (MC-ICPMS, Neptune, Thermo Scientific) at the Pole Spectrometrie Ocean (Ifremer, Brest). The purified Si solutions were diluted to 1 ppm using 1% nitric acid and introduced to the Neptune using an Apex HF desolvator to give a signal intensity of about 25 V on mass 28 at medium resolution. The concentration of HF in the standard (NBS28) and the samples was fixed (~1 mM HF) and the signal intensity matched within 10%. A matching amount of magnesium (1 ppm) was added to each sample and standard. The beam intensity on masses 28, 29, and 30 for silicon and on masses 25 and 26 for magnesium were monitored for a block of 30 cycles (8 s integrations), followed by 5 min of rinse with 1% HNO_3. The background signal intensity on mass 28 at the end of the rinse was in the order of 1% of the standard/sample signal intensity.

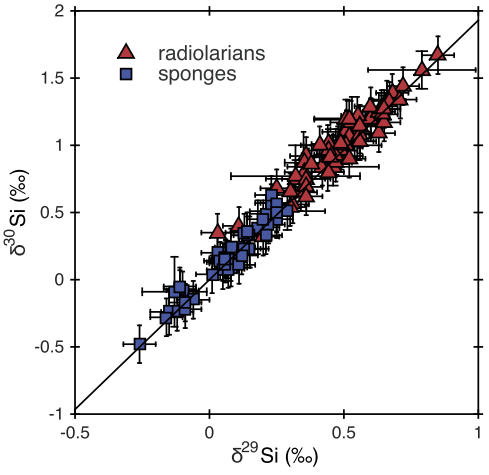

Fig. 2. Three-isotope plot of δ^{30}Si and δ^{29}Si values of radiolarian tests (red triangles) and sponge spicules (blue squares). The black line represents the expected mass-dependent fractionation ($\delta^{30}\text{Si} = 1.93 \times \delta^{29}\text{Si}$). Vertical and horizontal bars represent 1σ. (For interpretation of the references to colour in this figure, the reader is referred to the web version of this article.)

Si isotope ratios (^{29}Si/^{28}Si and ^{30}Si/^{28}Si) were corrected for internal mass bias using the Mg internal standard following the method prescribed by Cardinal et al. (2003). These corrected ratios were used to calculate δ^{30}Si and δ^{29}Si, averaged from two series of bracketed measurements (standard-sample-standard):

$$\delta^{x}\text{Si} = \left(\frac{R_{sam}}{R_{std}} - 1\right) \times 1000 \quad (1)$$

where R_{sam} and R_{std} are the corrected ratios of ^{x}Si/^{28}Si of the sample and the standard respectively. Values fall on the expected mass-dependent fractionation line $\delta^{30}\text{Si} = 1.93 \times \delta^{29}\text{Si}$ ($r^2 = 0.96$, $n = 112$; Fig. 2), implying the successful removal of all polyatomic interferences during measurement. Analysis of the secondary standards Diatomite and Big Batch prepared following identical protocols, in a different analytical session, yielded values in good agreement with accepted values (Reynolds et al., 2007; Supplementary Table 1). Long-term precision (expressed as 2σ) based on measurements of multiple NBS28 standards and secondary standards was of ±0.14‰ on δ^{30}Si and ±0.06‰ on δ^{29}Si.

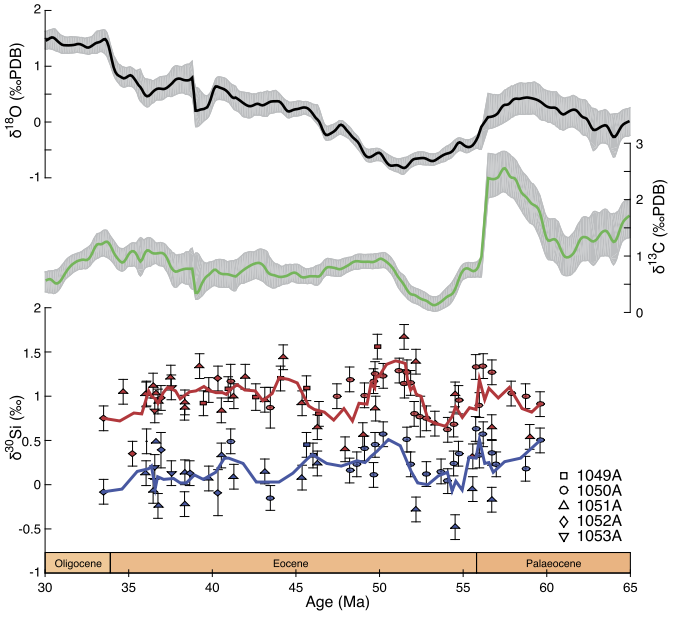

Fig. 3. Radiolarian tests (red symbols) and sponge spicules (blue symbols) δ^{30}Si values against sample age. Vertical bars show 1σ. Thick red and blue lines represent the three-points moving average for the radiolarian test and the sponge spicule records respectively. Stable carbon (green line) and oxygen (black line) isotopes in the North Atlantic from Cramer et al. (2009). Shaded areas show the 95% confidence interval. (For interpretation of the references to colour in this figure, the reader is referred to the web version of this article.)

3. Results

The 65 analysed radiolarian samples cover the period 59.6 to 33.5 Ma, with δ^{30}Si values ranging from +0.32 to +1.67‰ (mean of +0.99‰) and are consistently more positive than the 47 samples of monoaxonic sponge spicules (−0.48 to +0.63‰, with a mean of +0.17‰) over the same time interval (Fig. 3). All data are available in Supplementary Table 1.

Neither the radiolarian nor the sponge δ^{30}Si record shows a significant trend through time over the entire interval (−0.001‰ per Ma, $r^2 = 0.01$ for the radiolarian data, and +0.008‰ per Ma with $r^2 = 0.06$ for the sponge data). However, both datasets contain shorter time scale features, as shown most clearly in a 3-point running average (Fig. 3). In both the radiolarian and the sponge record, there is a positive excursion in δ^{30}Si between ca. 54 and 50 Ma of 0.7 and 0.5‰, respectively. This excursion is followed, between ca. 50 and 47 Ma, by a drop of 0.7‰ for the radiolarian record and of about 0.25‰ for the sponge record. It is worth noting that the difference in amplitude of the decrease between the two records might result from an artefact caused by the lower sampling resolution in the sponge dataset. The radiolarian record may show a second, less pronounced excursion from 47 to 43 Ma, although more samples are needed to confirm this. The sponge record over this interval is too sparse to show any excursion. After 43 Ma, both records appear to be fairly invariant with values of δ^{30}Si of $+1.04 \pm 0.05$‰ ($n = 19$) for the radiolarian record and $+0.10 \pm 0.24$‰ ($n = 17$) for the sponge spicule record.

The two records also appear to be broadly parallel. Calculation of the offset between radiolarian and sponge spicule δ^{30}Si over time is possible from paired sponge and radiolarian analyses from the same samples. The typical offset between the records is 0.82 ± 0.29‰ ($n = 41$) and shows no trend with sample age (Fig. 4).

4. Discussion

The reconstruction of ocean DSi concentrations over geological times has only been approached in a semi-quantitative manner.

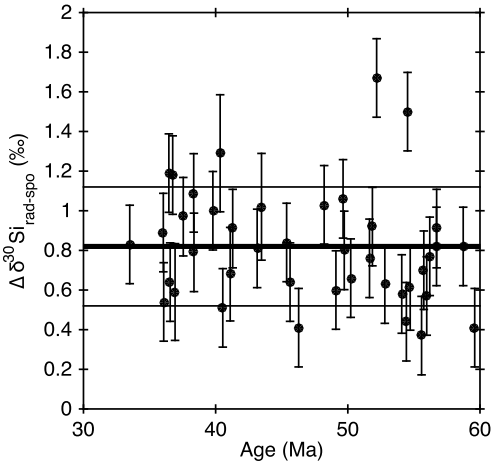

Fig. 4. Offset between radiolarian tests and sponge spicules δ^{30}Si through time. Thick line represents the mean and dashed lines show $\pm 1\sigma$.

The development of δ^{30}Si of marine sponge spicules as a proxy for DSi concentrations (Hendry et al., 2010; Wille et al., 2010) has opened the door to longer timescales studies (e.g. Egan et al., 2013). However, a major issue with this approach is the requirement that the silicon isotopic composition of the source DSi must be independently constrained. Here, we utilise the published $\Delta\delta^{30}$Si-[DSi] sponge spicule calibration (Hendry and Robinson, 2012) with a range of reasonable δ^{30}Si values for the ambient water. Our goal is to estimate the DSi concentration of waters bathing Blake Nose during the Palaeogene. In doing so, we provide the first quantitative constraints on DSi concentrations in the deep layer of the Palaeogene Atlantic. Specifically, we address (i) the probable range of DSi concentrations and δ^{30}Si at our site during the early to mid Palaeogene (section 4.1), (ii) the implications of these estimates in the context of previous studies (section 4.2) and (iii) what mechanisms may explain the (co-)variation in the radiolarian test and sponge spicule δ^{30}Si records (section 4.3). Given that we are among the first to apply this new proxy on these timescales, we end by explicitly addressing some possible concerns (section 4.4).

4.1. Reconstruction of DSi concentrations and δ^{30}Si

At a rudimentary level, it is noteworthy how similar the Palaeogene North Atlantic Si cycle as recorded in our sponge and radiolarian δ^{30}Si records is to the present day North Atlantic.

4.1.1. Surface waters

As with the majority of the global ocean, the modern North Atlantic (i.e. 0–60°N) is characterised by nearly entirely Si depleted surface waters (upper few hundred metres). The silicon isotope composition of the upper water column (<1000 m) encompassing the living habitat of radiolarians in the Atlantic ranges from +1.00‰ to +2.89‰ (Brzezinski and Jones, 2015; De La Rocha et al., 2000; de Souza et al., 2012). Assuming the fractionation of silicon isotopes during formation of radiolarian tests is ca. −1.5‰ (see section 4.4.4 for a discussion of this assumption), modern radiolarians should have $\delta^{30}Si_{rad}$ values spanning from −1.0‰ to +1.9‰. No modern data exist, but deglacial (~17 ka BP) radiolarians from the north Atlantic (33.7°N, −57.6°W) average 1.5‰ (Hendry et al., 2014), and Holocene radiolarians in two cores from the Atlantic sector of the Southern Ocean (49.0°S, 12.7°W and 52.6°S, 4.5°E) range from −0.45‰ to 1.17‰ (Abelmann et al., 2015). Our Palaeogene radiolarian $\delta^{30}Si_{rad}$ data broadly overlap with the published measurements, suggesting the $\delta^{30}Si_{DSi}$ of upper water column during the Palaeogene was similar or perhaps slightly ^{30}Si enriched as compared to modern values.

4.1.2. Bottom waters

In contrast to the other ocean basins, the deep waters (>1000 m) of the north Atlantic are relatively Si deplete, ranging from <15 μM in e.g. the Labrador Sea or the Iceland Basin, to a maximum of ~60 μM in the western equatorial Atlantic (Garcia et al., 2014). In contrast, bottom waters of the Pacific and Indian oceans are consistently >100 μM, ranging up to >170 μM in the North Pacific. The fundamental reason for this inter-basin gradient is that the modern North Atlantic is a site of deepwater formation, where Si depleted surface water is subducted and drawn southwards. Measurements of $\delta^{30}Si_{DSi}$ in modern Atlantic waters between 1500 and 2700 m (the approximate depth of modern sponge habitats along the Blake Nose transect) fall between 0.90–1.86‰ (De La Rocha et al., 2000; de Souza et al., 2012; Brzezinski and Jones, 2015).

Using modern DSi concentrations and the established relationship between DSi concentration ([DSi]) and the magnitude of siliceous sponge silicon isotope fractionation expressed as $\Delta\delta^{30}Si_{spg\text{-}DSi}$ (the difference in $\delta^{30}Si$ values of sponges and the source DSi; $\delta^{30}Si_{sponge} - \delta^{30}Si_{DSi}$) (Hendry and Robinson, 2012), we can estimate what $\delta^{30}Si$ value modern sponge spicules at Blake Nose might have. $\Delta\delta^{30}Si_{spg\text{-}DSi}$ has been empirically calibrated on sponge spicules from sediment coretops (Hendry and Robinson, 2012) as:

$$\Delta\delta^{30}Si_{spg\text{-}DSi} = -6.54 + \frac{270}{53 + [DSi]} \quad (2)$$

which can be rearranged to estimate the DSi concentration of the source water:

$$[DSi] = \frac{270}{\delta^{30}Si_{spg} - \delta^{30}Si_{DSi} + 6.54} - 53 \quad (3)$$

As captured in equations (2) and (3), the predicted magnitude of fractionation increases with increasing DSi concentration, ranging from −1.45 to −5.47‰ between 1 to 200 μM. Present-day DSi concentrations around Blake Nose are ca. 15–30 μM at a depth of 2500 m and imply a sponge silicon isotope fractionation ($\Delta\delta^{30}Si$) ranging from −2.6 to −3.3‰ (cf. equation (2)). Combined with the range of $\delta^{30}Si_{DSi}$ values measured in Atlantic waters, this equates to an expected modern sponge silicon isotope composition of ca. −2.4 to −0.6‰, with our best guesses ([DSi] = 20 μM, $\delta^{30}Si = +1.5$‰) equating to a $\delta^{30}Si_{spg}$ of −1.34‰. To our knowledge, no modern spicules have been measured in the vicinity of Blake Nose, but a record from 300 km to the north has recent (late Holocene) $\delta^{30}Si_{spg}$ values of ca. −1.2 to −1.5‰ (Hendry et al., 2014). Our sponge data reported here are consistently heavier, with a mean of +0.17‰. This first-order observation strongly suggests that Palaeogene DSi concentrations at Blake Nose were lower than modern values.

However, as captured in equations (2) and (3), there are two unknowns ([DSi] and $\delta^{30}Si_{DSi}$) and therefore there are no unique reconstructions of [DSi]. Essentially, our data can be explained by either low-[DSi], low-$\delta^{30}Si_{DSi}$ waters or high-[DSi], high-$\delta^{30}Si_{DSi}$ waters. This already hints at a more likely scenario: in the modern Atlantic (and the ocean as a whole), there is a negative relationship between [DSi] and $\delta^{30}Si_{DSi}$ (De La Rocha et al., 2000; de Souza et al., 2012, 2015; Brzezinski and Jones, 2015), making it hard to generate high-DSi, high $\delta^{30}Si_{DSi}$ waters. This is because the main process that increases seawater $\delta^{30}Si_{DSi}$ values (i.e. biological utilisation) also removes DSi, while the reverse is also true: increases in seawater [DSi] tend to lower its $\delta^{30}Si_{DSi}$ (i.e. by opal dissolution). This suggests that a low-[DSi], high-$\delta^{30}Si_{DSi}$ solution is more likely. We can test the robustness of the interpretation of low-DSi by reconstructing ambient water DSi concentrations with a range of increasingly implausible seawater $\delta^{30}Si_{DSi}$. Shown in Fig. 5a, we perform this exercise with steps in $\delta^{30}Si_{DSi}$ at 0.5‰ to

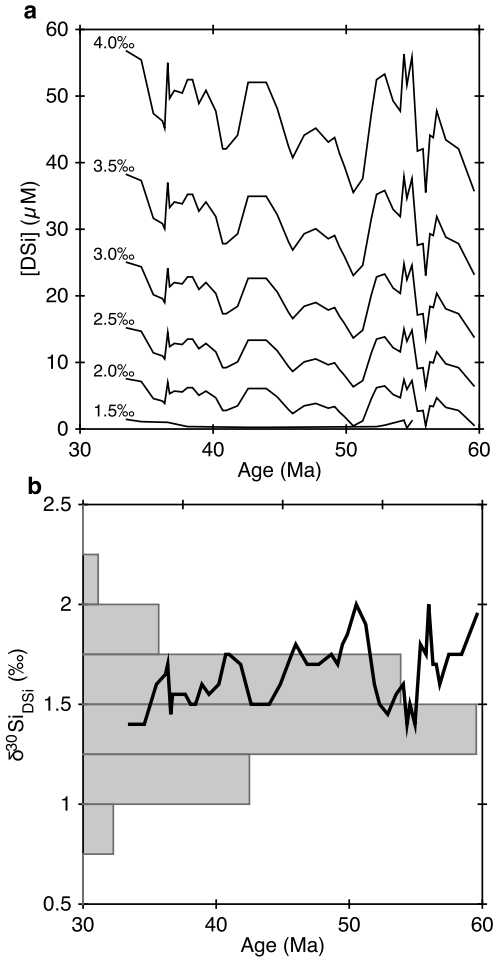

Fig. 5. (a) Reconstructed DSi concentrations according to fixed values of $\delta^{30}Si$ $\delta^{30}Si_{DSi}$. (b) Minimum $\delta^{30}Si_{DSi}$ values (black line) required to reconstruct DSi concentrations (i.e. [DSi] > 0 μM). The horizontal histogram represents the modern distribution of $\delta^{30}Si_{DSi}$ in the Atlantic below 1000 m.

a maximum of 4.5‰, greater than the maximum observed in the modern ocean (+4.4‰ in highly productive, DSi-deplete waters in the Peruvian upwelling zone; Grasse et al., 2013). Note that this is almost certainly a gross overestimation for bottom water DSi: the highest value to our knowledge for a water mass >1000 m depth is 2.2‰ in the Atlantic (De La Rocha et al., 2000), and <1.6‰ in other ocean basins. Maximum predicted DSi concentrations do not exceed 60 μM, but generally are <10 μM. These maximum reconstructed values of about 60 μM are relatively low compared to the previously estimated pre-Palaeogene concentrations (50–60 ppm, ca. 1000 μM; Siever 1991) or to the modern North Pacific where concentrations below 1000 m are typically between 100 and 200 μM (Garcia et al., 2014).

The point of this exercise is not to precisely define what the DSi concentrations of waters bathing Blake Nose were, but rather to demonstrate that even with improbable assumed $\delta^{30}Si_{DSi}$ (i.e. > 4‰), the reconstructed inputs are remarkably low (i.e <60 μM) throughout the early Palaeogene relative to those predicted by earlier work (see discussion below; Maliva et al., 1989).

A second useful outcome of this exercise is that it allows us to define the minimum bottom water $\delta^{30}Si_{DSi}$ value that produces meaningful results (namely [DSi] > 0 μM). As shown in Fig. 5b, this averages 1.65‰ throughout our study period, and never dips below 1.40‰. This is similar to the range of values seen in the North Atlantic today (Fig. 5b) but given that these are minimum values it

implies Palaeogene North Atlantic seawater DSi was slightly more ^{30}Si enriched than the present day.

4.2. Implications of silicon depleted bottom waters at Blake Nose

4.2.1. Extent of silicon depletion

It is first worth considering the extent to which our interpretations can be extrapolated beyond the Blake Nose escarpment itself. We suggest that our results argue for near-global DSi depletion in the surface ocean, and at least in the North Atlantic for deeper waters. The logic behind this conclusion is based on two simple premises. First, that the only way to generate DSi-deplete bottom water is to subduct DSi depleted surface waters, and second, that depletion of DSi from the surface ocean is unlikely to have been a localised phenomenon.

Premise 1 is why North Atlantic Deep Water (NADW) has low [DSi] (<20 μM) and Antarctic Bottom Water (AABW) is DSi replete (∼100 μM) (Garcia et al., 2014); NADW derives from low DSi waters while AABW does not. It follows that surface waters at the source of the bottom water (see below) that bathed Blake Nose were DSi depleted, and did not accumulate much DSi by remineralisation. By application of the second premise, the majority of the global surface ocean was also DSi deplete. Premise 2 can be validated from the modern ocean – with the exception of Fe limited regions like the Southern Ocean, DSi is uniformly low in the surface ocean (<10 μM). It is supported by the global distribution of the major groups of silicifying planktonic organisms in the early-mid Palaeogene: both radiolarians and diatoms were ubiquitous, meaning the North Atlantic was not unique. Further support for the extrapolation of our results to the regional scale (for intermediate/deep waters) and the global scale (for surface water) comes from the relative homogeneity within ocean basins with regards to DSi concentrations and the lack of any suitable mechanism for generating and maintaining a gradient of DSi concentrations. For example, from 1500 to 2500 m water depth in the north Atlantic DSi varies from 10 to 35 μM, and from 120 to 180 μM, in the North Pacific, i.e. consistency over a large area. This implies that DSi measured (or in our case reconstructed) at a point below the surface ocean can be reasonably extrapolated within the ocean basin in which it occurs.

4.2.2. Implications for evolution of ocean Si cycle on geological timescales

The conclusion that the sponge spicule record robustly yields low DSi concentrations for Blake Nose in the Palaeogene is in contrast to the established narrative. This argues for a transition from ocean DSi concentrations in the region of 1000 μM in the Cretaceous to <100 μM in the late Cenozoic due to the expansion of the diatoms (e.g. Siever, 1992). This was originally based on the sedimentary loci of different chert facies (Maliva et al., 1989), and has since found additional support from changes in radiolarian and silicoflagellate silicification (Lazarus et al., 2009; van Tol et al., 2012). Using a simple box model, De La Rocha and Bickle, 2005 suggested a diatom-mediated drawdown in DSi could take as little as ∼2.5 Ma. If such a decrease occurred in the early Cenozoic, siliceous sponges growing in this time should have shifted from producing highly fractionated (lower δ^{30}Si) to less fractionated (higher δ^{30}Si) spicules (Hendry and Robinson, 2012; Wille et al., 2010) that should produce a highly resolvable decrease in sponge spicule δ^{30}Si (of a few permil). Such a drop is absent in our data.

It is therefore helpful to look at the assumptions underlying the supposed early Cenozoic DSi drawdown. It is ascribed to the ecological success of diatoms (Maliva et al., 1989), specifically to their ability to produce and export high quantities of BSi even at low DSi concentrations, and premised on early work that argued for an almost exponential increase in diatom diversity though the Cenozoic (e.g. Small, 1950). However, reconstructing diatom diversity – assuming this is a reasonable proxy for their production – is complicated, and biases can easily be introduced (Kotrc and Knoll, 2015). Most attempts to define diatom diversification to date have used the Neptune database, and different approaches suggest either i) little net Cenozoic change with a slight late-Eocene peak (Cermeño et al., 2015; Rabosky and Sorhannus, 2009), ii) a general Cenozoic diversification (Lazarus et al., 2014; Spencer-Cervato, 1999) or iii) general stasis throughout the Cenozoic (Kotrc and Knoll, 2015). While our data cannot eliminate any of these possibilities, they do suggest that if the diatoms truly were responsible for a Cretaceous-Palaeogene DSi drawdown, they had developed the ability to achieve this prior to 60 Ma.

4.2.3. Implications for reconstructions of Palaeogene ocean circulation

The Early Cenozoic was a highly dynamic period of critical reorganisation of the Earth systems. Firstly, stable oxygen isotopes from benthic foraminifera show that the Earth was gradually transitioning from a greenhouse world in the Early Palaeogene towards an icehouse world (Zachos et al., 2001; Fig. 3). From the Early Eocene to the Eocene–Oligocene transition, temperatures decreased from 12 °C higher than present (the highest estimated temperatures over the whole Cenozoic) to low temperatures allowing the formation of ice on Antarctica (Zachos et al., 2001). Secondly, the global ocean circulation was experiencing major perturbations as inferred from stable carbon isotopes (e.g. Zachos et al., 2001; Cramer et al., 2009; Fig. 3). Cramer et al. (2009) show a high degree of carbon stable isotopes homogeneity between different ocean basins during the Early Palaeogene, representing a similar degree of accumulation of nutrients in all ocean basins (i.e. the same water "age") and a multitude of loci of deepwaters formation. The carbon stable isotope signature of the different basins differentiated from the Late Palaeogene and Neogene onwards, potentially resulting from the establishment and strengthening of the Antarctic Circumpolar Current (Cramer et al., 2009).

Our data provide two new insights. First, the sponge δ^{30}Si record is consistent throughout the depth profile of cores studied (ODP 1049–1052; 1300–2700 m), implying a single water mass was present at all of these sites. Second, they suggest the source of the water did not change during the period studied here (59.6 to 33.5 Ma) – or at least that it coincidentally had a δ^{30}Si-[DSi] pairing that produced similar spicule δ^{30}Si. Therefore, we need to identify a Palaeocene–Eocene source area for the bottom waters at Blake Nose that i) was DSi deplete at the time of formation, and ii) did not accumulate substantial amounts of regenerated DSi as it travelled from the its site of formation to Blake Nose.

Reconstructing the movement of water-masses through time is of considerable interest given the cause-and-effect feedbacks between global climate and ocean circulation. To this end, Nd isotope ratios (expressed as εNd) have been extensively employed. Briefly, this proxy is based on Nd's short residence time and heterogeneous distribution in the ocean, coupled with the fact that different source regions have distinctive εNd values related to the age and lithology of the material being weathered. This means dissolved Nd isotope ratios reflect their source via continental weathering (Lacan et al., 2012), and are transferred to e.g. fish debris early in the diagenetic process (Staudigel et al., 1985), so Nd isotope analysis of leachates from this material reflects εNd of the deep water in the region – and therefore the source of the water mass.

In the early Palaeogene, εNd values of ca. −11 are found at Demerara Rise in the tropical North Atlantic (∼9°N, MacLeod et al., 2011). Contemporaneous values from the South Atlantic were more radiogenic (εNd ≈ −8; Via and Thomas, 2006), but Fe–Mn

crusts in the waters forming in the Nordic seas had εNd of ~ -9 to -11 (O'nions et al., 1998), leading MacLeod et al. (2011) to suggest that the deep waters of the early Cenozoic tropical Atlantic had a North Atlantic source, termed Northern Component Water (NCW). Via and Thomas (2006) had previously demonstrated that water reaching Walvis Ridge ($\sim$30°S) began to take on a North Atlantic character early in the Oligocene ($\sim$30 Ma), coincident with sedimentological evidence for intensified deep water formation in the North Atlantic (e.g. Davies et al., 2001), suggesting that the evolution of modern North Atlantic Deep Water (NADW) might have proceeded as a two-step process (MacLeod et al., 2011). However, the interpretation of NCW influencing the Equatorial Atlantic during the Palaeogene has been contested on the basis of uncertainties in the εNd values of coeval north Atlantic waters (e.g. Robinson and Vance, 2012). Ocean circulation models (Bice and Marotzke, 2002; Lunt et al., 2010), inferences based on carbon isotope (δ^{13}C) gradients in benthic foraminifera (Borrelli et al., 2014; Corfield and Norris, 1996; Nunes and Norris, 2006) and sedimentological evidence (Mountain and Miller, 1992) also tend to prefer a Southern deep water source for the western North Atlantic for most of the Palaeogene.

Nd isotope evidence from Blake Nose itself is sparse. In the late Cretaceous, prior to our δ^{30}Si records, εNd ≈ -8 (MacLeod et al., 2008) similar to contemporaneous values from the South Atlantic (Robinson et al., 2010) and consistent with a South Atlantic source through the Central Atlantic Gateway. Two samples from the carbon isotope excursion of the Palaeocene–Eocene Thermal Maximum (PETM; 55.5 Ma) at site 1050 provided εNd of -8.34 and -9.17 (Thomas et al., 2003), also lower than dissolved Nd in the modern Nordic or Labrador seas (Lacan et al., 2012).

Overall, it seems the most likely source of waters bathing Blake Nose during the early-mid Palaeogene derived from the south, though the issue is far from settled. Another intriguing possibility is the presence of a low-latitude, Tethyan deep water mass formed by evaporation-induced density increases, termed Warm Saline Deep Water (WSDW; Norris et al., 2001; Pak and Miller, 1992), which has gained some support from εNd data (Scher and Martin, 2004), although it has proved difficult to reproduce in modelling studies.

The dynamics of water subduction and advection in thek Palaeocene–Eocene southern high latitudes were not analogous to present. Prior to the development of the Antarctic Circumpolar Current (ACC) the region was likely dominated by water sinking, while post-ACC, the opening of ocean gateways allowed wind driven upwelling along the Antarctic Divergence, increasing deep water formation in the North Atlantic and setting the scene for the evolution of the modern state of ocean overturning. This led Egan et al. (2013) to posit the presence of a pre-Late Eocene southern overturning loop, causing the poleward advection of nutrient deplete surface waters. The low nutrient status of these surface waters may conceivably have been augmented by the absence of (modern) Fe limitation at high southern latitudes via Fe inputs from an unglaciated Antarctica.

Therefore, the Southern Ocean is a plausible source of bottom water for the Palaeocene–Eocene Blake Nose, if these waters had low [DSi] (Egan et al., 2013). However, previous sponge analysis on ODP core 689 (Southern Ocean, Atlantic sector) spanning the Eocene–Oligocene boundary, though only slightly overlapping with the end of our records (De La Rocha, 2003; Egan et al., 2013; Fig. 3) exhibit δ^{30}Si values about 1.5‰ lower than the Blake Nose record, implying correspondingly greater DSi concentrations (cf. Equations (2)–(3)), which would argue against a southern source for Blake Nose bottom waters. The long travel distance for this water source also suggests that it would accumulate more regenerated DSi than our reconstructions allow, as evidenced by Palaeocene benthic δ^{13}C gradients (Borrelli et al., 2014; Cramer et al., 2009). We therefore favour a Tethyan WSDW, given the much lower distance available for regeneration of DSi from sinking BSi. Extending the Blake Nose sponge δ^{30}Si record forwards, and the Southern Ocean records of De La Rocha (2003) and Egan et al. (2013) backwards, would resolve this issue and shed considerable light on the development of the modern Atlantic circulation.

4.3. Co-variation between radiolarian and sponge δ^{30}Si

The radiolarian and sponge δ^{30}Si records behave similarly over the Palaeocene–Eocene (Figs. 3 and 4). This is not necessarily an intuitive result: these two groups of silicifiers occupy different environments and have different Si uptake mechanisms, meaning there is little *a priori* reason why they should co-vary. This suggests a major control on both the radiolarian and sponge δ^{30}Si records is the silicon isotope composition of the ambient seawater. The total variability in our sponge spicule and radiolarian records is about 0.5‰ and 0.7‰, respectively, in the smoothed curves (Fig. 3). For context, changes in diatom or sponge δ^{30}Si associated with the transition from the last glacial maximum to the Holocene are of similar amplitudes (e.g. Ehlert et al., 2013; recently reviewed in Frings et al., 2016).

Such long-term co-variation can be explained in two ways. The first explanation is a localised shift in δ^{30}Si of both bottom and surface water DSi, related to changes in ocean circulation maintained over several millions of years. The alternative is a whole ocean change in mean δ^{30}Si, related to a change in the average silicon isotopic composition of DSi inputs to the ocean (Frings et al., 2016). Given that the Nd isotope evidence (e.g. Via and Thomas, 2006) does not suggest large-scale reorganisation of Atlantic circulation during the early Palaeogene, we outline some mechanisms by which the inputs to the ocean Si cycle may have varied.

The largest input of silicon to the ocean is river DSi, which is ultimately derived from the chemical weathering of continental silicate minerals (Tréguer and De La Rocha, 2013) and today has an average δ^{30}Si value around $+1.0$–$+1.5$‰ (Frings et al., 2016). It is generally accepted that silicate weathering rates are linked to climate, and thus act as a planetary thermostat (Walker et al., 1981). Over long time scales carbon mass-balance imposes the constraint that the consumption of CO_2 via weathering of silicate minerals balances the degassing of CO_2 from the solid Earth (Berner and Caldeira, 1997), assuming silicate weathering is the most important sink in the global C cycle. If this is assumed to be proportional to the seafloor spreading rate – thought to be broadly invariant over the past 180 Ma (Rowley, 2002) – this requires that net CO_2 consumption by silicate weathering rates over the same period have also been relatively consistent, transient changes in the size of the Earth's surficial carbon pool notwithstanding. However, the ratio of fluvial DSi produced to CO_2 consumed is not fixed, and depends both on the cation content of the silicate minerals undergoing weathering, and the congruency of the weathering reactions (i.e. the degree of completeness of the conversion of minerals into solutes). Indeed, because the primary control on river DSi is thought to be the extent of Si incorporated into secondary clay minerals (De La Rocha et al., 2000; Frings et al., 2016), then this provides a simple mechanism for varying the magnitude of the river DSi flux and its silicon isotopic composition: vary the efficiency with which silicate weathering converts the parent minerals to solutes.

Proxy data indicates higher Palaeocene–Eocene atmospheric pCO_2 and temperature reconstructions from marine and terrestrial settings and climate models indicate elevated early Cenozoic warmth (e.g. Zachos et al., 2001). Maintaining a hotter, higher pCO_2 world but with the same CO_2 removal therefore requires that the relationship between pCO_2 and silicate weathering rate dif-

fers from todays, i.e. a less efficient continental weathering regime. There is no relationship between weathering rate and river δ^{30}Si, so the impact on the δ^{30}Si of riverine DSi is hard to predict. A 9‰ Cenozoic increase in ocean lithium isotope ratios (Misra and Froelich, 2012), which are also sensitive to continental weathering congruency, has been interpreted as a global decrease in weathering congruency over the Cenozoic (i.e. a greater proportion of Li tied up in secondary clays, and attributed to lower relief continents mantled with thick, cation-depleted soils (Misra and Froelich, 2012). Although Si isotopes also respond to weathering congruency, it is not clear if have the same sensitivity. Frings et al. (2015) show that the lowland alluvial plain in the Ganges tends to increase river δ^{30}Si, while lowland regions that are more sediment starved tend to produce lower river δ^{30}Si (e.g. Hughes et al., 2013). Frings et al. (2016) argue that there is enough potential variability in the continental Si cycle to shift ocean δ^{30}Si by up to 0.8‰ on millennial timescales; the same must be on longer timescales, and so may explain some of the trends apparent in the radiolarian and sponge spicule δ^{30}Si data. It remains to be understood how the continental Si cycle, including weathering, varied throughout the Cenozoic, especially in the face of various external perturbations. These include periods of extended volcanism and important steps in the evolution of the terrestrial biosphere. Although we have focused on the fluvial DSi flux, a series of hypotheses regarding variations in the other DSi sources to the ocean (chiefly groundwater DSi and atmospheric and fluvial sediment dissolution) could also be constructed (cf. Frings et al., 2016). The salient point here is that changes in mean ocean δ^{30}Si of >0.5‰, via changes in the magnitude and δ^{30}Si of the ocean Si inputs, are feasible, and that long-term marine δ^{30}Si records – especially if and when they become more abundant – offer a novel way to explore the interactions between climate and weathering.

4.4. Alternative explanations

Our interpretation of a Si depleted North Atlantic during the early Cenozoic (section 4.1) and an ocean silicon isotope budget controlled by variations in the inputs (section 4.3) parsimoniously explains all the available observations. However, other interpretations are conceivable. In the following, we briefly explore issues that are known to affect other geochemical proxies hosted in biominerals (namely dissolution/diagenesis, local effects, environment/proxy calibration problems, and ecological effects), and suggest future work where necessary.

4.4.1. Dissolution and diagenesis

The magnitude of Si isotope fractionation associated with dissolution of BSi is unclear. In an initial set of experiments, Demarest et al. (2009) identified a fractionation factor of -0.55‰, i.e. a tendency to discriminate against the release of the heavier isotopes of approximately half the magnitude of the fractionation associated with BSi production by diatoms (De La Rocha et al., 1997). However, later work was unable to reproduce these findings (Wetzel et al., 2014). Core-top diatom BSi δ^{30}Si from the Southern Ocean also agreed well with mixed layer filtered diatom samples, implying little to no effect of dissolution and early diagenesis on opal δ^{30}Si values (Egan et al., 2012), a conclusion supported by water column studies (Fripiat et al., 2011). Similarly, Panizzo et al. (2016) show the absence of silicon isotope fractionation during 1600 m of sinking of freshwater diatoms. Both Wetzel et al. (2014) and Demarest et al. (2009) emphasise that a large proportion of the initial BSi is required to dissolve in order that a resolvable isotope fractionation is visible in the residual material, yet our own observations and those of others (Sanfillipo and Blome, 2001; Witkowski et al., 2014) suggest the BSi is excellently preserved. We also note that as dissolution is a surface process, mass-balance requires that any putative fractionation cannot be maintained indefinitely; the outer (^{30}Si enriched) layer will also dissolve, with the net result that the δ^{30}Si of the DSi solubilised will equal that of the original opal.

The ODP shipboard lithostratigraphy indicates the episodic occurrence of porcellanite, particularly in poorly recovered sections in the middle Eocene. Porcellanite is a form of opal-CT, an initial step on the diagenetic pathway of biogenic silica to chert. Tatzel et al. (2015) have shown that this transformation – which proceeds by a dissolution/reprecipitation reaction – is associated with silicon isotope fractionation, the manifestation of which depends on the completeness of transformation. While this is problematic for interpreting δ^{30}Si of cherts, it is unlikely to be an issue for our data: individual microfossils were handpicked and observation by both light microscopy and scanning electron microscopy did not reveal any signs of dissolution or crystallisation. In general, the fact that we observe two distinct and variable populations of δ^{30}Si (i.e. radiolarians and sponges; Fig. 3) together in the sediment also argues against any diagenetic overprinting or equilibration. Analysis by X-Ray Diffractometer (XRD) of early Eocene sediments in hole 1051B produces a broad peak characteristic of amorphous silica (Frings, unpublished data). Overall, it is likely artefacts introduced by dissolution or diagenesis are minimal.

4.4.2. Local effects

During at least the middle Eocene, diatom assemblages from hole 1051 (Witkowski et al., 2014) were often dominated by species interpreted as neritic (shallow water), implying considerable offshore transport by surface currents. Diatom taxa with inferred benthic habitats (*Actinoptychus*, *Diplomenora*, *Mastogloia* and *Rhaphoneis*) are also present in 1051 (Witkowski et al., 2014). If the sponge spicules are also being laterally transported, they could be recording a coastal environment signal rather than a deep-water signal, diminishing the scope of our interpretations (section 4.1). However, the dominant taxa *Paralia*, *Pseudopodosira* and *Rutilaria* inferred as neritic or tychoplanktonic by Witkowski et al. (2014), frequently occur in the Neptune database in decidedly pelagic settings. Therefore, although these species are most commonly interpreted as neritic, their habitat might not have been limited to near shore environments but may have extended further away from the coast. We also note that Blake Nose Eocene benthic foraminifera are typical of paleodepths between 1000–2000 m (Borrelli et al., 2014). Extensive input of allochthonous material is also counter to the sedimentology of Blake Nose (Benson et al., 1978), and the absence of substantial amounts of terrestrial siliciclastic material that would indicate large-scale offshore sediment transfer. Further, the benthic diatom taxa reported contribute a very minor fraction of the total assemblage data of Witkowski et al. (2014). We therefore summarise that the evidence for significant post-depositional lateral transport of sponge spicules is limited, and that the δ^{30}Si signal derives from the reported palaeodepths of the cores (Table 1), not a proximal upslope environment. Future work might seek to verify this through relating sponge assemblages to depth habitats.

Lateral transport might be of greater importance for the radiolarians. However, independently of their distance from the coast, our interpretation of the radiolarian signal remains unchanged. As developed in section 4.1.1, radiolarians give us an estimation of the Si isotopic composition of seawater, which was apparently very similar to modern values during the Palaeogene.

4.4.3. Proxy-environment calibration

The possibility of a relationship between sponge silicon isotope fractionation and ambient DSi concentrations was first posited almost simultaneously by Wille et al. (2010) and Hendry et al. (2010), and expanded on by Hendry and Robinson (2012) who developed the hyperbolic-form calibration of Eqn. (2). Current un-

derstanding of this relationship attributes it to the ratio of Si influx to Si efflux to and from sponge sclerocyte (spicule forming) cells, both with associated fractionations, and that it is this ratio that is controlled by ambient DSi concentrations (Wille et al., 2010; Hendry and Robinson, 2012). As a palaeoceanographic proxy, sponge silicon isotopes are still in their infancy relative to e.g. well-established calcite based proxies, and scientific understanding will undoubtedly become more nuanced. Sponge δ^{30}Si suffers from the same fundamental limitation as many other (bio)geochemical proxies: we must assume the proxy-environment calibration based on modern sponges from previous studies is valid in the early Cenozoic. Yet we find it unlikely that the basic tenet of the calibration will change. It has been demonstrated that the observed relationship is not driven by temperature, pH, salinity, or the concentration of other nutrients (Hendry and Robinson, 2012; Wille et al., 2010). The calibration used here (Eqn. (2)) is based on coretop spicules, but agrees well with data from living sponges of the classes Demospongiae and Hexactinellida (Hendry and Robinson, 2012; Hendry et al., 2010; Wille et al., 2010), the two dominant groups of Si-producing sponges. In sponges, putative sclerocyte cells have been reported in Precambrian fossils (Li et al., 1998), and sponge morphology has been remarkably consistent (Pisera, 2006), arguing for a reasonably consistent relationship between [DSi] and $\Delta\delta^{30}$Si.

4.4.4. Ecological effects on radiolarian Si isotope fractionation

Knowledge regarding silicon isotope fractionation by radiolarians is still at an early stage, partly due to the difficulties involved in successfully culturing radiolarians. Their silicification is poorly understood but thought to occur within a specialised cryptoplasma membrane termed the cytokaymma, which is involved in regulating internal Si concentrations and guiding Si precipitation (Wallace et al., 2012). The extent to which radiolarians have the Si efflux mechanisms that cause Si isotope fractionation to vary with DSi concentration (as in sponges) is unclear. Overall, it seems fractionation should be related only to fractionation during the initial uptake of DSi and its transport into the cell, as is the case with diatoms. This is supported by studies that demonstrate a constant offset (albeit variable between regions) between δ^{30}Si of diatoms and radiolarians (Abelmann et al., 2015; Hendry et al., 2014). (Note that while it has long been assumed that diatom fractionation is independent of ambient DSi concentrations, compilations of all available data (Hendry and Robinson, 2012; Abelmann et al., 2015) suggest there may be a relationship, albeit muted relative to sponges). Thus, in the absence of evidence to the contrary, we assume here that $\delta^{30}Si_{rad}$ reflects the isotopic composition of the source DSi with an offset due to fractionation. Note that this assumption makes little difference to our conclusions regarding ocean Si depletions, which are based on the sponge δ^{30}Si data.

The actual magnitude of this fractionation is also unknown. Hendry et al. (2014) used an offset of −1.1 to −2.1‰ between radiolarian silica and DSi in the Sargasso Sea, consistent with previous estimates (Egan et al., 2012) in order to model seawater δ^{30}Si during the most recent Heinrich Stadial (17 ka). Abelmann et al. (2015) used a similar range of fractionation of −0.8 to −1.5‰ for their reconstructions based on coretop samples. However, robust data underpinning these values is lacking. Radiolarians dwell in the upper several hundred meters of the water column. Interestingly, the 125–250 µm and >250 µm size fractions of radiolarians in the deglacial Southern Ocean differ in their silicon isotopic composition by >1‰ (Abelmann et al., 2015). It is unclear what is causing this, although the two most likely suggestions are either that i) the species dominating each size fraction grow at different depths in the water column and/or time of the year, and so tap different sources of DSi and/or ii) the fractionation factor associated with radiolarian BSi production varies with species or growth rate/ontogeny. More data from paired plankton and water samples and/or culturing experiments are needed to shed light on this.

5. Conclusions

We have analysed the silicon isotopic composition of the remains of siliceous organisms (radiolarians and sponges) from the Blake Nose escarpment in the western North Atlantic, spanning 60 to 33 Ma. Our study highlights the potential of combining δ^{30}Si values from sponge spicules and radiolarian tests to infer aspects of the Si cycle in the geological past. Using these data, in particular the sponge δ^{30}Si values, we provide the first quantitative estimates of ocean DSi concentrations in the early Cenozoic. Our results indicate that, contrary to previous work, the North Atlantic was not DSi replete during the Palaeocene–Eocene. We cannot define if and when a drawdown of DSi concentrations occurred in this region of the ocean although it must have occurred prior to 60 Ma. We suggest that the timing and ubiquity of the various steps that have been proposed for the evolution of ocean DSi concentrations since the end of the Precambrian must be reconsidered. The observation of low-DSi waters bathing Blake Nose helps constrain past ocean circulation. Further investigations, primarily on the extent of Si isotope fractionation by radiolarians, as well as from different ocean basins would be beneficial to help put the data in a global context and to begin to elucidate more clearly the linkages between climate and the Si cycle.

Acknowledgements

This work was funded by a grant from the Knut and Alice Wallenberg Foundation to DJC plus support from a LEFEC/CYBER grant ('SiMS') to CDLR. KRH was funded by the Royal Society. We thank Emmanuel Ponzevera at IFREMER and Carolina Funkey at Lund University for laboratory assistance, and Nathalie van der Putten, also at Lund, for providing the necessary equipment for microfossil separation. We thank Damien Cardinal, two anonymous reviewers, and AE Martin Frank for their constructive comments that helped to improve this manuscript.

Appendix A. Supplementary material

Supplementary material related to this article can be found online at http://dx.doi.org/10.1016/j.epsl.2016.08.006.

References

Abelmann, A., Gersonde, R., Knorr, G., Zhang, X., Chapligin, B., Maier, E., Esper, O., Friedrichsen, H., Lohmann, G., Meyer, H., 2015. The seasonal sea-ice zone in the glacial Southern Ocean as a carbon sink. Nat. Commun. 6.

Benson, W.E., Sheridan, R.E., Pastouret, L., Enos, P., Freeman, T., Murdmaa, I.O., Worstell, P. (eds.), Gradstein, F., Schmidt, R.R., Weaver, F.M., Stuermer, D.H., 1978. Initial reports of the Deep Sea Drilling Project.

Berner, R.A., Caldeira, K., 1997. The need for mass balance and feedback in the geochemical carbon cycle. Geology 25, 955.

Bice, K.L., Marotzke, J., 2002. Could changing ocean circulation have destabilized methane hydrate at the Paleocene/Eocene boundary? Paleoceanography 17.

Borrelli, C., Cramer, B.S., Katz, M.E., 2014. Bipolar Atlantic deepwater circulation in the middle-late Eocene: effects of Southern Ocean gateway openings. Paleoceanography 29, 308–327.

Brzezinski, M.A., Jones, J.L., 2015. Coupling of the distribution of silicon isotopes to the meridional overturning circulation of the North Atlantic Ocean. Deep-Sea Res. Part 2. Top. Stud. Oceanogr. 116, 79–88.

Cardinal, D., Alleman, L.Y., de Jong, J., Ziegler, K., André, L., 2003. Isotopic composition of silicon measured by multicollector plasma source mass spectrometry in dry plasma mode. J. Anal. At. Spectrom. 18, 213–218.

Cermeño, P., Falkowski, P.G., Romero, O.E., Schaller, M.F., Vallina, S.M., 2015. Continental erosion and the Cenozoic rise of marine diatoms. Proc. Natl. Acad. Sci. 112, 4239–4244.

Corfield, R.M., Norris, R.D., 1996. Deep water circulation in the Paleocene ocean. Geol. Soc. (Lond.) Spec. Publ. 101, 443–456.

Cramer, B., Toggweiler, J., Wright, J., Katz, M., Miller, K., 2009. Ocean overturning since the Late Cretaceous: inferences from a new benthic foraminiferal isotope compilation. Paleoceanography 24.

Davies, R., Cartwright, J., Pike, J., Line, C., 2001. Early Oligocene initiation of North Atlantic deep water formation. Nature 410, 917–920.

De La Rocha, C.L., Brzezinski, M.A., DeNiro, M.J., 1997. Fractionation of silicon isotopes by marine diatoms during biogenic silica formation. Geochim. Cosmochim. Acta 61, 5051–5056.

De La Rocha, C., Brzezinski, M.A., DeNiro, M., Shemesh, A., 1998. Silicon-isotope composition of diatoms as an indicator of past oceanic change. Nature 395, 680–683.

De La Rocha, C.L., 2003. Silicon isotope fractionation by marine sponges and the reconstruction of the silicon isotope composition of ancient deep water. Geology 31, 423.

De La Rocha, C.L., Bickle, M.J., 2005. Sensitivity of silicon isotopes to whole-ocean changes in the silica cycle. Mar. Geol. 217, 267–282.

De La Rocha, C.L., Brzezinski, M.A., DeNiro, M.J., 2000. A first look at the distribution of the stable isotopes of silicon in natural waters. Geochim. Cosmochim. Acta 64, 2467–2477.

de Souza, G.F., Reynolds, B.C., Rickli, J., Frank, M., Saito, M.A., Gerringa, L.J.A., Bourdon, B., 2012. Southern Ocean control of silicon stable isotope distribution in the deep Atlantic Ocean. Glob. Biogeochem. Cycles 26, GB2035.

de Souza, G.F., Slater, R.D., Hain, M.P., Brzezinski, M.A., Sarmiento, J.L., 2015. Distal and proximal controls on the silicon stable isotope signature of North Atlantic Deep Water. Earth Planet. Sci. Lett. 432, 342–353.

Demarest, M.S., Brzezinski, M.A., Beucher, C.P., 2009. Fractionation of silicon isotopes during biogenic silica dissolution. Geochim. Cosmochim. Acta 73, 5572–5583.

Egan, K.E., Rickaby, R.E.M., Hendry, K.R., Halliday, A.N., 2013. Opening the gateways for diatoms primes Earth for Antarctic glaciation. Earth Planet. Sci. Lett. 375, 34–43.

Egan, K.E., Rickaby, R.E.M., Leng, M.J., Hendry, K.R., Hermoso, M., Sloane, H.J., Bostock, H., Halliday, A.N., 2012. Diatom silicon isotopes as a proxy for silicic acid utilisation: a Southern Ocean core top calibration. Geochim. Cosmochim. Acta 96, 174–192.

Ehlert, C., Grasse, P., Frank, M., 2013. Changes in silicate utilisation and upwelling intensity off Peru since the Last Glacial Maximum – insights from silicon and neodymium isotopes. Quat. Sci. Rev. 72, 18–35.

Engström, E., Rodushkin, I., Baxter, D.C., Öhlander, B., 2006. Chromatographic purification for the determination of dissolved silicon isotopic compositions in natural waters by high-resolution multicollector inductively coupled plasma mass spectrometry. Anal. Chem. 78, 250–257.

Frings, P.J., Clymans, W., Fontorbe, G., Christina, L., Conley, D.J., 2016. The continental Si cycle and its impact on the ocean Si isotope budget. Chem. Geol. 425, 12–36.

Frings, P.J., Clymans, W., Fontorbe, G., Gray, W., Chakrapani, G.J., Conley, D.J., De La Rocha, C., 2015. Silicate weathering in the Ganges alluvial plain. Earth Planet. Sci. Lett. 427, 136–148.

Fripiat, F., Cavagna, A.-J., Savoye, N., Dehairs, F., André, L., Cardinal, D., 2011. Isotopic constraints on the Si-biogeochemical cycle of the Antarctic Zone in the Kerguelen area (KEOPS). Mar. Chem. 123, 11–22.

Garcia, H., Locarnini, R., Boyer, T., Antonov, J., Baranova, O., Zweng, M., Reagan, J., Johnson, D., 2014. World Ocean Atlas 2013, volume 4: Dissolved Inorganic Nutrients (Phosphate, Nitrate, Silicate). S. A. Mishonov Technical Ed., pp. 1–25.

Grasse, P., Ehlert, C., Frank, M., 2013. The influence of water mass mixing on the dissolved Si isotope composition in the Eastern Equatorial Pacific. Earth Planet. Sci. Lett. 380, 60–71.

Griffiths, J.D., Barker, S., Hendry, K.R., Thornalley, D.J., Flierdt, T., Hall, I.R., Anderson, R.F., 2013. Evidence of silicic acid leakage to the tropical Atlantic via Antarctic Intermediate Water during Marine Isotope Stage 4. Paleoceanography 28, 307–318.

Hendry, K., Swann, G.E., Leng, M.J., Sloane, H.J., Goodwin, C., Berman, J., Maldonado, M., 2015. Technical note: silica stable isotopes and silicification in a carnivorous sponge Asbestopluma sp. Biogeosciences 12, 3489–3498.

Hendry, K.R., Georg, R.B., Rickaby, R.E.M., Robinson, L.F., Halliday, A.N., 2010. Deep ocean nutrients during the Last Glacial Maximum deduced from sponge silicon isotopic compositions. Earth Planet. Sci. Lett. 292, 290–300.

Hendry, K.R., Robinson, L.F., 2012. The relationship between silicon isotope fractionation in sponges and silicic acid concentration: modern and core-top studies of biogenic opal. Geochim. Cosmochim. Acta 81, 1–12.

Hendry, K.R., Robinson, L.F., McManus, J.F., Hays, J.D., 2014. Silicon isotopes indicate enhanced carbon export efficiency in the North Atlantic during deglaciation. Nat. Commun. 5.

Hughes, H.J., Sondag, F., Santos, R.V., André, L., Cardinal, D., 2013. The riverine silicon isotope composition of the Amazon Basin. Geochim. Cosmochim. Acta 121, 637–651.

Kotrc, B., Knoll, H.A., 2015. Morphospaces and databases: diatom diversification through time. In: Hamm, C. (Ed.), Evolution of Lightweight Structures: Analyses and Technical Applications. Springer, Netherlands, Dordrecht, pp. 17–37.

Lacan, F., Tachikawa, K., Jeandel, C., 2012. Neodymium isotopic composition of the oceans: a compilation of seawater data. Chem. Geol. 300, 177–184.

Lazarus, D., Barron, J., Renaudie, J., Diver, P., Türke, A., 2014. Cenozoic planktonic marine diatom diversity and correlation to climate change. PloS ONE 9, e84857.

Lazarus, D.B., Kotrc, B., Wulf, G., Schmidt, D.N., 2009. Radiolarians decreased silicification as an evolutionary response to reduced Cenozoic ocean silica availability. Proc. Natl. Acad. Sci. 106, 9333–9338.

Li, C.-W., Chen, J.-Y., Hua, T.-E., 1998. Precambrian sponges with cellular structures. Science 279, 879–882.

Lunt, D.J., Valdes, P.J., Jones, T.D., Ridgwell, A., Haywood, A.M., Schmidt, D.N., Marsh, R., Maslin, M., 2010. CO_2-driven ocean circulation changes as an amplifier of Paleocene–Eocene thermal maximum hydrate destabilization. Geology 38, 875–878.

MacLeod, K., Londoño, C.I., Martin, E., Berrocoso, Á.J., Basak, C., 2011. Changes in North Atlantic circulation at the end of the Cretaceous greenhouse interval. Nat. Geosci. 4, 779–782.

MacLeod, K.G., Martin, E.E., Blair, S.W., 2008. Nd isotopic excursion across Cretaceous ocean anoxic event 2 (Cenomanian–Turonian) in the tropical North Atlantic. Geology 36, 811–814.

Maliva, R.G., Knoll, A.H., Siever, R., 1989. Secular change in chert distribution: a reflection of evolving biological participation in the silica cycle. Palaios, 519–532.

Misra, S., Froelich, P.N., 2012. Lithium isotope history of Cenozoic seawater: changes in silicate weathering and reverse weathering. Science 335, 818–823.

Morley, D.W., Leng, M.J., Mackay, A.W., Sloane, H.J., Rioual, P., Battarbee, R.W., 2004. Cleaning of lake sediment samples for diatom oxygen isotope analysis. J. Paleolimnol. 31, 391–401.

Mountain, G.S., Miller, K.G., 1992. Seismic and geologic evidence for early Paleogene deepwater circulation in the western North Atlantic. Paleoceanography 7, 423–439.

Norris, R., Klaus, A., Kroon, D., 2001. Mid-Eocene deep water, the Late Palaeocene thermal maximum and continental slope mass wasting During the Cretaceous–Palaeogene impact. Geol. Soc. (Lond.) Spec. Publ. 183, 23–48.

Norris, R.D., Kroon, D., Klaus, A., et al., 1998. Proc. ODP, Init. Repts., 171B: College Station, TX (Ocean Drilling Program).

Nunes, F., Norris, R.D., 2006. Abrupt reversal in ocean overturning during the Palaeocene/Eocene warm period. Nature 439, 60–63.

O'nions, R., Frank, M., Von Blanckenburg, F., Ling, H.-F., 1998. Secular variation of Nd and Pb isotopes in ferromanganese crusts from the Atlantic, Indian and Pacific Oceans. Earth Planet. Sci. Lett. 155, 15–28.

Pak, D.K., Miller, K.G., 1992. Paleocene to Eocene benthic foraminiferal isotopes and assemblages: implications for deepwater circulation. Paleoceanography 7, 405–422.

Panizzo, V.N., Swann, G.E.A., Mackay, A.W., Vologina, E., Sturm, M., Pashley, V., Horstwood, M.S.A., 2016. Insights into the transfer of silicon isotopes into the sediment record. Biogeosciences 13, 147–157.

Pisera, A., 2006. Palaeontology of sponges–a review. Can. J. Zool. 84, 242–261.

Rabosky, D.L., Sorhannus, U., 2009. Diversity dynamics of marine planktonic diatoms across the Cenozoic. Nature 457, 183–186.

Reynolds, B.C., Aggarwal, J., André, L., Baxter, D., Beucher, C., Brzezinski, M.A., Engström, E., Georg, R.B., Land, M., Leng, M.J., 2007. An inter-laboratory comparison of Si isotope reference materials. J. Anal. At. Spectrom. 22, 561–568.

Robinson, S.A., Murphy, D.P., Vance, D., Thomas, D.J., 2010. Formation of "Southern Component Water" in the Late Cretaceous: evidence from Nd-isotopes. Geology 38, 871–874.

Robinson, S.A., Vance, D., 2012. Widespread and synchronous change in deeppocean circulation in the North and South Atlantic during the Late Cretaceous. Paleoceanography 27.

Rowley, D.B., 2002. Rate of plate creation and destruction: 180 Ma to present. Geol. Soc. Am. Bull. 114, 927–933.

Sanfilippo, A., Blome, C.D., 2001. Biostratigraphic implications of mid-latitude Palaeocene–Eocene radiolarian faunas from Hole 1051A, ODP Leg 171B, Blake Nose, western North Atlantic. Geol. Soc. (Lond.) Spec. Publ. 183, 185–224.

Scher, H.D., Martin, E.E., 2004. Circulation in the Southern Ocean during the Paleogene inferred from neodymium isotopes. Earth Planet. Sci. Lett. 228, 391–405.

Siever, R., 1992. The silica cycle in the Precambrian. Geochim. Cosmochim. Acta 56, 3265–3272.

Small, J., 1950. Quantitative evolution: XVI. Increase of species-number in diatoms. Ann. Bot. 14, 91–113.

Spencer-Cervato, C., 1999. The Cenozoic deep sea microfossil record: explorations of the DSDP/ODP sample set using the Neptune database. Palaeontol. Electronica 2, 270.

Staudigel, H., Doyle, P., Zindler, A., 1985. Sr and Nd isotope systematics in fish teeth. Earth Planet. Sci. Lett. 76, 45–56.

Tatzel, M., von Blanckenburg, F., Oelze, M., Schuessler, J.A., Bohrmann, G., 2015. The silicon isotope record of early silica diagenesis. Earth Planet. Sci. Lett. 428, 293–303.

Thomas, D.J., Bralower, T.J., Jones, C.E., 2003. Neodymium isotopic reconstruction of late Paleocene–early Eocene thermohaline circulation. Earth Planet. Sci. Lett. 209, 309–322.

Tréguer, P.J., De La Rocha, C.L., 2013. The world ocean silica cycle. Annu. Rev. Marine Sci. 5, 477–501.

van Tol, H.M., Irwin, A.J., Finkel, Z.V., 2012. Macroevolutionary trends in silicoflagellate skeletal morphology: the costs and benefits of silicification. Paleobiology 38, 391–402.

Via, R.K., Thomas, D.J., 2006. Evolution of Atlantic thermohaline circulation: early Oligocene onset of deep-water production in the North Atlantic. Geology 34, 441–444.

Walker, J.C., Hays, P., Kasting, J., 1981. A negative feedback mechanism for the long-term stabilization of the Earth's surface temperature. J. Geophys. Res. 86, 9776–9782.

Wallace, A.F., Wang, D., Hamm, L.M., Knoll, A.H., Dove, P.M., 2012. Eukaryotic skeletal formation. In: Knoll, A.H., Canfield, D.E., Konhauser, K.O. (Eds.), Fundamentals of Geobiology. John Wiley & Sons, Ltd, Chichester, pp. 150–187.

Wetzel, F., De Souza, G., Reynolds, B., 2014. What controls silicon isotope fractionation during dissolution of diatom opal? Geochim. Cosmochim. Acta 131, 128–137.

Wille, M., Sutton, J., Ellwood, M.J., Sambridge, M., Maher, W., Eggins, S., Kelly, M., 2010. Silicon isotopic fractionation in marine sponges: a new model for understanding silicon isotopic variations in sponges. Earth Planet. Sci. Lett. 292, 281–289.

Witkowski, J., Bohaty, S.M., Edgar, K.M., Harwood, D.M., 2014. Rapid fluctuations in mid-latitude siliceous plankton production during the Middle Eocene Climatic Optimum (ODP Site 1051, western North Atlantic). Mar. Micropaleontol. 106, 110–129.

Zachos, J., Pagani, M., Sloan, L., Thomas, E., Billups, K., 2001. Trends, rhythms, and aberrations in global climate 65 Ma to present. Science 292, 686–693.